MAGNETIC RESONANCE IN MEDICINE 7, 262–279 (1988)

High-Resolution ^{1}H NMR Spectral Signature from Human Atheroma*

JUSTIN D. PEARLMAN,†‡ JAROSLAV ZAJICEK,§¶ MICHAEL B. MERICKEL,‖ CHARLES S. CARMAN,‖ CARLOS R. AYERS,† JAMES R. BROOKEMAN,‖,** AND MICHAEL F. BROWN§,††

*Departments of †Internal Medicine, ‖Biomedical Engineering, and **Radiology, University of Virginia School of Medicine, Charlottesville, Virginia 22908, and §Department of Chemistry and Biophysics Program, University of Virginia, Charlottesville, Virginia 22901*

Received May 6, 1987; revised October 26, 1987

Coronary artery disease due to atherosclerosis takes the lives of approximately 550,000 Americans each year—an enormous toll. Put in economic terms, the cost to the United States alone has been estimated to exceed 60 *billion* dollars annually. We have found that well-resolved proton (^{1}H) NMR spectra can be obtained from human atheroma (fatty plaque), despite its macroscopic solid appearance. The fraction of the total spectral intensity corresponding to the sharp ^{1}H NMR signals is temperature dependent and approaches unity at body temperature (37°C). Studies of the total lipids extracted from atheroma and cholesteryl esters were conducted to identify the chemical and physical origin of the spectral signature. The samples were characterized through assignment of their chemical shifts and by measurement of their T_1 and T_2^* relaxation times as a function of magnetic field strength. The results suggest that the relatively sharp ^{1}H NMR signals from human atheroma (excluding water) are due to a mixture of cholesteryl esters, whose liquid-crystalline to isotropic fluid phase transition is near body temperature. Preliminary applications to NMR imaging of human atheroma are reported, which demonstrate early fatty plaque formation within the wall of the aorta. These findings offer a basis for noninvasive imaging by NMR to monitor early and potentially reversible stages of human atherogenesis.

INTRODUCTION

Atherosclerosis is the leading cause of death and debility in the United States and other Western industrialized nations. Its presence is often first identified by the occurrence of heart attack, stroke, renal failure, or sudden death. Nearly one of every three Americans can expect to suffer from the consequences of this disease (*1*). The early lesions in blood vessel walls are marked by clinically silent, intra- and extracellular

* Presented at 59th American Heart Association Meeting, Dallas, Texas, November 1986 (J. D. Pearlman *et al., Circulation* **74,** II–202 (1986)), and 31st Annual Biophysical Society Meeting, New Orleans, Louisiana, February 1987 (J. Zajicek *et al., Biophys. J.* **51,** 78a (1987)).

‡ Present address: Cardiac Group, Massachusetts General Hospital, Bulfinch 4, Boston, MA 02114.

¶ Permanent address: Institute of Organic Chemistry and Biochemistry, Czechoslovak Academy of Sciences, 166 10 Prague 1, Czechoslovakia.

†† To whom correspondence should be addressed at present address: Department of Chemistry, University of Arizona, Tucson, AZ 85721.

0740-3194/88 $3.00

accumulations of cholesterol and cholesteryl esters, as well as triglycerides, phospholipids, and various lipoproteins (*2–5*). The lipids deposited between the intima and media of the arterial wall are believed to originate mainly from serum low-density lipoproteins (LDL),[1] which transport cholesterol within the body in the form of cholesteryl esters (*3–7*). Epidemiological studies (*8*), drug trials (*9, 10*), and biochemical studies (*6, 7, 11, 12*) have all implicated cholesterol and saturated fats of dietary and endogenous origin in the etiology of atherosclerosis (*3–5*). Dietary polyunsaturated fats, by contrast, are associated with reduced LDL cholesterol levels (*13, 14*) and lower incidence of cardiovascular disease (*15–18*). Lipids accumulating within the arterial wall may initiate the atherosclerotic process in response to injury of the blood vessel endothelium, followed by release of chemotactic substances, attraction of monocytes which ingest further lipids to become foam cells, and agglutination of platelets. Growth factors can then stimulate smooth muscle cells to migrate to the subendothelial area, which differentiate into fibroblasts, leading to synthesis of collagen, fibrosis, and eventual calcification (*3–5*). The clinical end results of atherosclerosis are caused by thrombosis or occlusion of the diseased vessels due to arterial plaque, thereby reducing or eliminating the supply of blood to key tissues and organs, such as the heart or brain.

Beyond this, little is known with certainty of the means by which lipids accumulate within the intima and media of the arterial wall, a process beginning often in childhood or early adolescence (*2–5*). As a result, strategies for prevention of atherosclerosis have met with limited success—particularly when conflicting with individual lifestyles, societal norms, and powerful economic interests. The availability of sensitive, noninvasive methods for monitoring of atherogenesis, in conjunction with more effective regimens for treatment of susceptible individuals, would represent a significant step forward (*1*). In particular, it seems worthwhile to pursue development of techniques for accurately identifying and quantifying the lipid constituents of atherosclerotic plaque (*2, 19–22*) within human arterial vessels, which mark early and potentially reversible (*23*) disease stages. Cholesteryl esters, the major class of lipids in atheromatous tissue (*2, 19–22*), comprise free cholesterol condensed with a carboxylic acid such as linoleate (18:2ω6), oleate (18:1ω9), palmitate (16:0), or arachidonate (20:4ω6). They are liquid-crystalline materials and are capable of undergoing thermotropic transitions among distinct intermediate phases between the liquid and solid states. Previous investigators have shown that high-resolution, ^{13}C NMR spectra can be acquired from the lipids of intact (*ex vivo*) atherosclerotic lesions of human and animal origin (*24–26*), and have conducted high-resolution ^{13}C and ^{1}H NMR studies of serum lipoproteins (*27–35*). To our knowledge, however, ^{1}H NMR spectroscopy of human arterial tissue has

[1] The following abbreviations and notation are used in this article: carbon-13, ^{13}C; 3-hydroxy-3-methylglutaryl coenzyme A, HMG CoA; low-density lipoprotein, LDL; magnetic resonance imaging, MRI; nuclear magnetic resonance, NMR; proton, ^{1}H; sodium 2,2-dimethyl-2-silapentane-5-sulfonate, DSS. Fatty acids are referred to by the standard notation *X*:*Y*ω*Z*, where *X* denotes the number of carbon atoms in the acyl chain, *Y* the number of double bonds, and *Z* the number of carbon atoms counting from the terminal methyl group to the last double-bonded atom. Arachidonic acid is denoted as 20:4ω6; linoleic acid as 18:2ω6; oleic acid as 18:1ω9; and palmitic acid as 16:0. The predominant cholesteryl esters found in human atheroma are referred to as cholesteryl arachidonate, CA; cholesteryl linoleate, CL; cholesteryl oleate, CO; and cholesteryl palmitate, CP; free cholesterol is denoted by CH.

not been reported. In view of the central role of ^1H in NMR imaging (*36, 37*), this would appear to be a promising avenue of investigation. Here we show that ^1H NMR spectroscopy can provide a high-resolution signature of human atheroma within the wall of the aorta. Chemical and physical information regarding the lipid constituents of arterial plaque is acquired; the results provide a quantitative basis for NMR imaging of early changes in human arterial walls due to atherogenesis.

EXPERIMENTAL SECTION

Samples of human arterial tissue were obtained freshly postmortem in conjunction with autopsies conducted at the University of Virginia Hospital. Intact diseased wall, subintimal atheroma, gruel plaque from ulcerated lesions, and control samples of normal arterial wall were removed by dissection of aorta specimens. Their composition was verified by subsequent quantitative thin-layer chromatography, by gas–liquid chromatography, and by histologic methods (*19–22*). Pure anhydrous cholesteryl esters, triolein, and cholesterol were obtained from Sigma (St. Louis, MO) and were used as received. All materials were kept under an argon atmosphere to minimize oxidation and were stored at 4°C. The data reported for cholesteryl esters refer to samples cooled from the isotropic liquid state (*38*).

^1H NMR studies were conducted at external magnetic field strengths of 6.342, 8.481, and 11.75 T (^1H frequencies of 270.0, 361.1, and 500.1 MHz). All of the ^1H NMR spectra shown in this article were acquired at 361.1 MHz, and the large residual water proton signal near 4.63 ppm was suppressed by selective radiofrequency saturation except during data acquisition; no first-order phase correction was applied. The chemical shifts are in parts per million (ppm) relative to an external capillary containing DSS. The spectra were typically acquired using single radiofrequency pulses of duration 2 μs, with a repetition time of 2 s; 50–1000 free induction decays were acquired in quadrature with Bessel filters and were Fourier transformed using 16K data points and a line broadening of 0.5 Hz. The total spectral width was $\pm$70 kHz ($\pm$194 ppm) (acquisition delay = 28 μs; dwell time = 7 μs). Spin–spin or transverse (T_2^*) relaxation times of the resolved resonances were estimated by fitting the spectra to Lorentzian lineshapes using the relation $T_2^* = (\pi\Delta\nu)^{-1}$, where $\Delta\nu$ is the full width at half-height (*36*). Spin–lattice or longitudinal (T_1) relaxation times were measured without saturation of the water proton signal using the inversion–recovery pulse sequence (*36*). NMR images were obtained with a Siemens Magnetom 1.0 T whole-body imager, operated at a magnetic field strength of 0.35 T, using the standard spin-warp with spin-echo method (*37*); individual planar slices were selectively excited. A surface coil of diameter 11 cm was used as a receive-only antenna to acquire the cross-sectional images of intact human aorta specimens located within a glass cylinder.

RESULTS AND DISCUSSION

High-resolution proton NMR spectra are obtained of human arterial plaque. Most arterial lesions can be classified in order of severity as fatty streaks, fatty plaque or intermediate lesions, fibrous plaque, gruel plaque, and complex lesions (*2–5, 19–22*). The severity of the lesions parallels the progression of lipid deposition within the arterial wall (*2, 20*). Fatty streaks comprise a phospholipid liquid-crystalline phase saturated with cholesterol and cholesteryl esters, coexisting with a second, oily or

liquid-crystalline phase of cholesteryl ester droplets. Fatty plaque and fibrous plaque contain the two preceding phases, together with a third phase of free cholesterol monohydrate crystals. In the more advanced lesions, lipids in the above three phases are associated with scar formation, calcification, and thrombosis (blood clot). We reasoned that despite its macroscopic, solid appearance, the presence of extracellular and intracellular cholesteryl esters in fatty plaque (*2, 20–22, 39, 40*), with relatively low isotropic to liquid-crystalline phase transition temperatures (*38*), could lead to sharp ^{1}H NMR spectra as seen for other isotropic fluids. In particular, we were interested in whether accumulations of cholesteryl esters and other lipids could be detected which form early atheroma within the walls of human arterial blood vessels (*2–5, 19–22*).

As a first step toward evaluating the biologic and chemical conditions necessary to obtain ^{1}H NMR spectra of fatty plaque, we studied excised human aortic tissue specimens with and without atheroma. Intact samples of aortic wall stripped of the tunica adventitia, microdissected subintimal fatty plaque, and total lipid extracts (*19–22*) of fatty plaque were investigated. The samples were obtained from eight subjects, aged 23 to 97 years, at times ranging from 15 min to 17 h after autopsy. Representative ^{1}H NMR spectra, obtained at body temperature (37°C) from a sample of freshly excised human atheroma (fatty plaque) suspended in deuterated buffer, are shown in Fig. 1. The sharply resolved spectral lines are identified in Fig. 1A and are assigned to the protons of the tertiary methyl ($C\underline{H}_3$) (0.70 ppm), secondary methyl ($C\underline{H}_3$) (0.87 ppm), aliphatic methylene [$(C\underline{H}_2)_n$] (1.27 ppm), methine ($C\underline{H}$) (1.27 to 2.25 ppm), allylic methylene ($=CH-C\underline{H}_2$) (1.99 to 2.18 ppm), doubly allylic methylene ($=CH-C\underline{H}_2-CH=$) (2.73 ppm), and vinyl ($=C\underline{H}-$) (5.28 ppm) groups of the fatty acyl chains and cholesterol rings of the atheromatous lipids (*41, 42*). Most of the observed intensity is contained in the narrow, well-resolved resonances, as evidenced by Fig. 1B, which shows the ^{1}H NMR spectrum of the same sample plotted over a larger range (−70 to +70 kHz), together with vertical expansions of the baseline regions. The sharp signal in Fig. 1B corresponds to the expansion of Fig. 1A; underlying broad spectral components are not seen. The vinyl, doubly allylic, and allylic resonances (Fig. 1A) are due largely to the unsaturated and polyunsaturated fatty acyl chains of the atheromatous lipid molecules, which include cholesteryl esters, triglycerides, and phospholipids, whereas the methylene and secondary methyl proton resonances also include contributions from lipids with saturated acyl chains. The sterol moieties of the atheromatous cholesteryl esters contribute to the methylene peak and give rise to methine and tertiary methyl proton resonances (*41, 42*). Thus, information is obtained regarding the chemical composition of intact atheroma *ex vivo,* that is, within the aortic wall. Distinct resonances attributable to the polar head groups and glycerol backbones of phospholipids and triglycerides were not identified.

In addition to excised human atheroma, samples of lyophilized (freeze-dried) atheroma, its extracted lipids, and control samples of normal intima–medial arterial wall were studied, all of which were suspended in deuterated buffer (Fig. 2). By lyophilization, one can further reduce the magnitude of the large water proton signal, thereby more clearly revealing resonances from other constituents of the arterial plaque. Similar ^{1}H NMR spectra are obtained from lyophilized fatty plaque (Fig. 2A) and total extracts of its lipids (Fig. 2B) as from atheroma *ex vivo,* whereas ^{1}H NMR spectra of control samples of normal intima–medial aortic wall (Fig. 2C) do not yield well-resolved

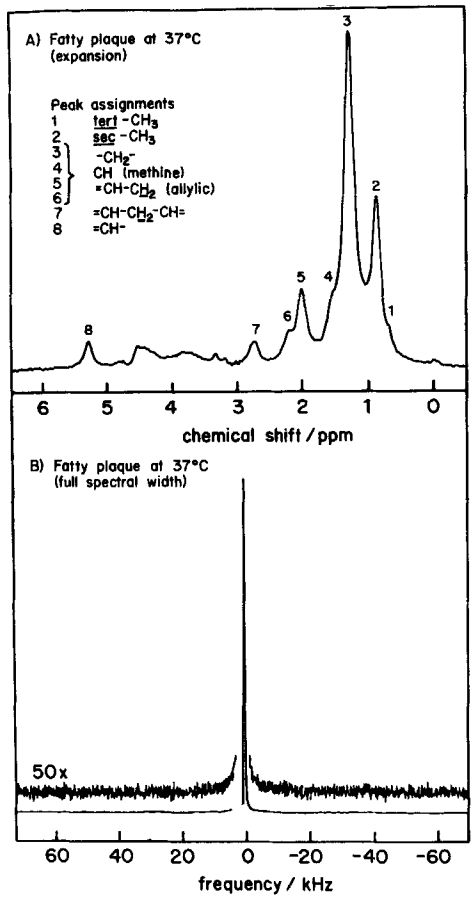

FIG. 1. High-resolution ^{1}H NMR spectra of human atheroma (fatty plaque) obtained at 37°C (body temperature). The spectra were acquired at a magnetic field strength of 8.481 T (resonance frequency of 361.1 MHz). The sample was suspended in deuterated buffer and the residual water proton peak at 4.63 ppm was suppressed selectively by radiofrequency irradiation. An expansion of the chemical-shift range from −0.5 to +6.5 ppm relative to DSS is shown in (A), and the full spectral width from −70 to +70 kHz in frequency units is shown in (B). In (A), the observed spectral lines are assigned as indicated to the lipid constituents of the arterial plaque. In (B), the ^{1}H NMR spectrum of the same sample is shown over a larger frequency range, together with 50-fold vertical expansions to either side of the sharp resonances; note the flat baseline and the absence of an underlying broad signal. Such high-resolution ^{1}H NMR spectra are typical of fluids, whereas human fatty plaque is macroscopically solid in appearance (see text).

spectral lines. Thus, the sharp resonances of human atheroma (fatty plaque) at 37°C are most likely due to accumulated lipids within the arterial wall. On a molar basis, the spectra reflect mainly the presence of cholesteryl esters, with minor contributions from triglycerides and phospholipids (*19–22*).

^{1}H NMR spectra of human atheroma have also been obtained as a function of temperature, and representative data are included in Fig. 3. Similar results are observed for extracts of the total atheromatous lipids (not shown). The intensities of the well-

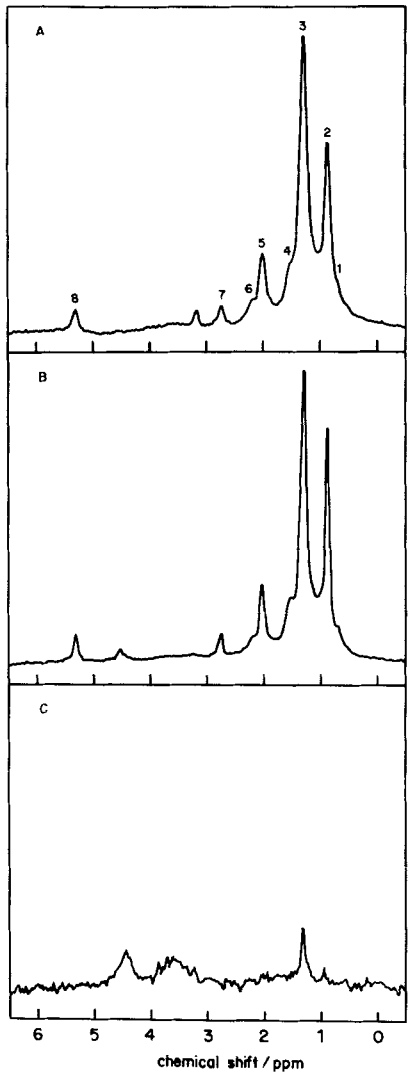

FIG. 2. Representative ^{1}H NMR spectra of arterial wall constituents obtained at 37°C. Expansions of the −0.5 to +6.5 ppm spectral region containing the sharp resonances are shown; little or no underlying broad components are observed in the same spectra plotted over a larger frequency range. In (A) is shown a ^{1}H NMR spectrum of a sample of lyophilized (freeze-dried) atheroma in deuterated buffer, different from that of Fig. 1, together with peak assignments. In (B) a ^{1}H NMR spectrum of the corresponding total extracted lipids containing deuterated buffer is depicted. Finally, in (C) is shown a ^{1}H NMR spectrum of a control sample of excised, nonatheromatous aortic wall in deuterated buffer, excluding adventitial fat, which was deemed not to contain significant atheroma by visual inspection; here the lipid resonances are much smaller. The high-resolution ^{1}H NMR spectra of atheroma thus appear to largely arise from the lipid constituents of fatty plaque.

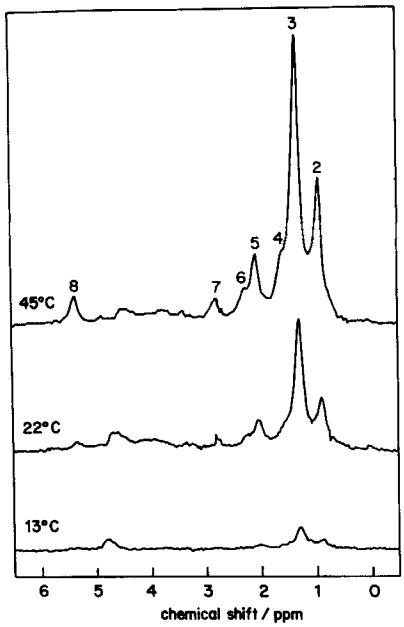

FIG. 3. Temperature dependence of ^{1}H NMR spectra of human atheroma (fatty plaque). Representative expansions of the −0.5 to +6.5 ppm chemical-shift range containing the observed resonances are shown plotted at the same vertical scale. With decreasing temperature, the fraction of the total signal corresponding to the sharp ^{1}H NMR spectral components decreases, indicative of a thermotropic transition of the lipid constituents near body temperature (37°C).

resolved peaks are maximal at temperatures above 37°C, suggesting that most or all of the total signal is observed. Below body temperature, a reversible decrease in the peak amplitudes is seen, indicating that a transition to a broader spectrum occurs whose breadth exceeds the range depicted; similar results have been obtained with ^{13}C NMR spectroscopy (*24, 26*). At sufficiently low temperatures, essentially no high-resolution ^{1}H NMR spectrum is found (Fig. 3). Since broad ^{1}H NMR spectra are characteristic of solids and liquid crystals (*43, 44*), the results of Fig. 3 suggest that the atheromatous cholesteryl esters undergo an isotropic to liquid-crystalline phase transition below body temperature. This conclusion is in agreement with X-ray diffraction and polarized light microscopy studies (*20, 39, 40*), which suggest that cholesteryl esters can exist within the intima and media of the arterial wall as small droplets (*2, 20, 39, 40*), due to their low solubility in other arterial tissue constituents (*38*). The results of ^{1}H NMR spectroscopy show clearly that the cholesteryl ester molecules of atheromatous lesions exist mainly in the isotropic liquid phase at body temperature, or near the onset temperature of their transition to the liquid-crystalline state (*24, 26, 39, 40*). These findings may have biological implications, since there is evidence that the physical state of cholesteryl esters (*38*) influences enzymatic activities, lipid transport, and lipid storage, which are important in atherogenesis (*11, 19, 20, 45*).

Proton NMR spectroscopy of cholesteryl esters and model lipid mixtures. The ^{1}H NMR lineshapes of biologically important cholesteryl esters in different physical states

(*19, 38*) were then investigated, including their liquid-crystalline mesophases, to identify further the chemical and physical basis for the observed spectral signature of human atheroma. At one extreme is the crystalline or solid phase, present at low temperatures; at the other is the isotropic or liquid phase, which is found at higher temperatures. The cholesteric and smectic liquid-crystalline mesophases occur at intervening temperatures (*38*) and represent intermediate states of molecular organization, in which the molecules are less highly ordered than in the solid or crystalline phase. The most abundant cholesteryl esters of atheromatous tissue (fatty plaque) are those of linoleate, oleate, palmitate, and arachidonate (*19–22*), which are present at molar ratios of approximately 10:8:3:3. The former three cholesteryl esters undergo monotropic transitions when cooled from the isotropic phase at temperatures depending on the length and degree of unsaturation of their fatty acyl chains (*38*), namely 36°, 48°, and 84°C, respectively; cholesteryl arachidonate melts inantiatropically at 19°C. The presence of small amounts of triglycerides, as found in human atheroma (*19–22*), is known to reduce the temperatures at which cholesteryl esters and their mixtures undergo transitions from the isotropic phase to the liquid-crystalline state (*19, 20, 38, 46, 47*).

The predominant cholesteryl esters found in arterial plaque (*19–22*) were studied over a range of temperatures spanning their known thermotropic transitions, as shown in Fig. 4. Representative data for anhydrous cholesteryl palmitate (CP) are depicted on the left (Figs. 4A–4D), which illustrate the ^{1}H NMR spectra found for each of the distinct phases of the cholesteryl esters. In the isotropic phase (90°C) (Fig. 4A), a high-resolution ^{1}H NMR spectrum is obtained, with sharp, approximately Lorentzian lineshapes (not shown). Only in the isotropic phase are the ^{1}H NMR spectral lines sharply defined, as in the spectra of human atheroma at 37°C, allowing identification of separate resonances from the protons of the methyl, aliphatic methylene, methine, singly and doubly allylic, and vinyl groups (cf. Fig. 1A). In the isotropic liquid phase, the areas under each of the resolved spectral peaks are proportional to the numbers of protons in the corresponding chemical environments. By contrast, for cholesteryl palmitate in the cholesteric (81°C) and smectic (77°C) liquid-crystalline states, and in the crystalline phase (22°C), relatively broad, non-Lorentzian ^{1}H NMR spectral lineshapes are obtained (Figs. 4B–4D). The observed non-Lorentzian lineshapes reflect largely the presence of residual static ^{1}H magnetic dipolar interactions (*43, 44*), which broaden the spectra and obscure the individual, chemically shifted resonances. On the right (Figs. 4E–4H) are shown ^{1}H NMR spectra at 37°C of cholesteryl linoleate (CL), cholesteryl oleate (CO), cholesteryl palmitate (CP), and free cholesterol (CH). Of the lipids investigated, only cholesteryl linoleate, the predominant cholesteryl ester of atheromatous tissue, exists in the isotropic phase at body temperature (*38*) and is found to give rise to a high-resolution ^{1}H NMR spectrum (Fig. 4E).

The thermal behavior of mixtures of the biologically important cholesteryl esters was then investigated, to determine whether the ^{1}H NMR spectra of human atheroma (Figs. 1–3) could be reproduced by its lipid constituents. With decreasing temperature, the sharp, liquid-phase spectra were gradually replaced by broader ^{1}H NMR spectra, due to the liquid-crystalline state (not shown). We reasoned that the presence of triglycerides, as found in human atheroma (*19–22*), may depress the transition temperatures of mixtures of cholesteryl esters (*20, 38, 46, 47*), leading to liquid-like ^{1}H NMR spectra at body temperature. This hypothesis was tested by conducting ^{1}H NMR studies

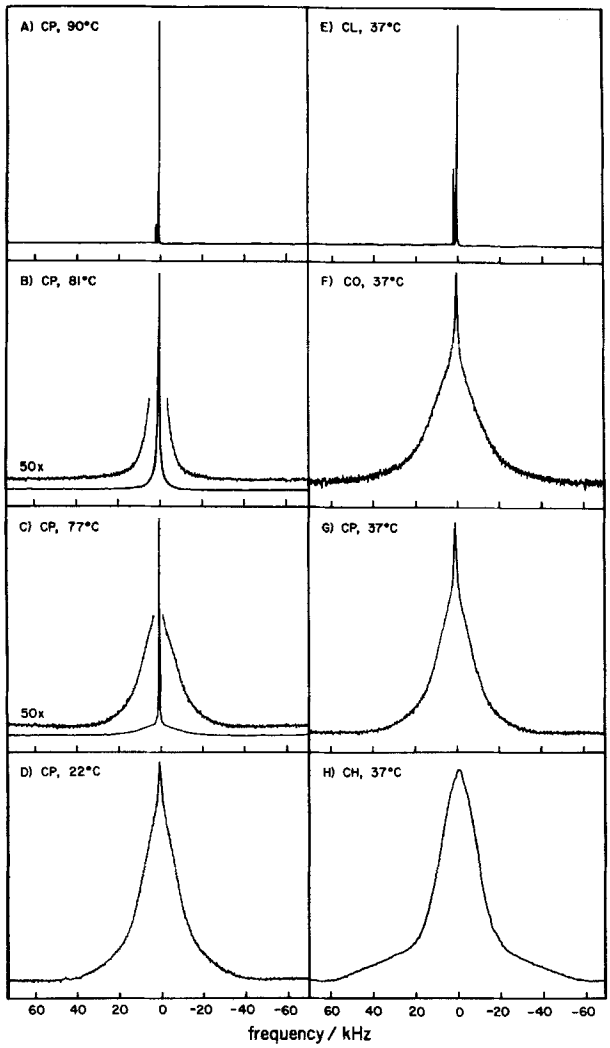

FIG. 4. ^{1}H NMR spectra of lipids found in human arterial plaque. The spectra are shown over a −70- to +70-kHz frequency range, together with 50-fold vertical expansions where indicated. At left (A–D) are shown ^{1}H NMR spectra of anhydrous cholesteryl palmitate (abbreviated CP) as a function of temperature. In (A) the isotropic liquid phase at 90°C, sharp spectral lines are obtained with no underlying broad component. In (B) the cholesteric liquid-crystalline phase at 81°C, (C) the smectic liquid-crystalline phase at 77°C, and (D) the crystalline solid phase at 22°C, broad, non-Lorentzian lineshapes are evident. Similar results are obtained for other cholesteryl esters with different transition temperatures (not shown). At right (E–H) are shown ^{1}H NMR spectra at 37°C of anhydrous cholesteryl linoleate (CL), cholesteryl oleate (CO), and cholesteryl palmitate (CP), as well as free cholesterol (CH). Cholesteryl linoleate is in the isotropic fluid phase at body temperature and gives rise to a sharp ^{1}H NMR spectrum (E). At 37°C, (F) cholesteryl oleate, (G) cholesteryl palmitate, and (H) free cholesterol are in the crystalline phase and yield broader ^{1}H NMR spectra. The broad lines in the crystalline and liquid-crystalline phases are due to residual ^{1}H magnetic dipolar interactions, which are averaged to zero in the isotropic liquid phase, leading to sharp ^{1}H NMR spectra.

of anhydrous mixtures of CL/CO/CP (molar ratios of 10:8:2) with and without triglycerides (Fig. 5). In the presence of 5 wt% triolein (Figs. 5A–5B), a sharp ^{1}H NMR spectrum is observed at 37°C, similar to that of human atheroma (Figs. 1A, 2A) and its extracted lipids (Fig. 2B), but with somewhat narrower lines. By contrast, if triolein is omitted from the mixture of cholesteryl esters (Figs. 5C–5D), then broader spectra are obtained at 37°C. Similar results have been obtained previously from ^{13}C NMR studies of mixtures of cholesteryl esters (*47, 48*).

The above results allow one to conclude that the sharp ^{1}H NMR spectra of human atheroma largely reflect the presence of cholesteryl esters which exist in the isotropic

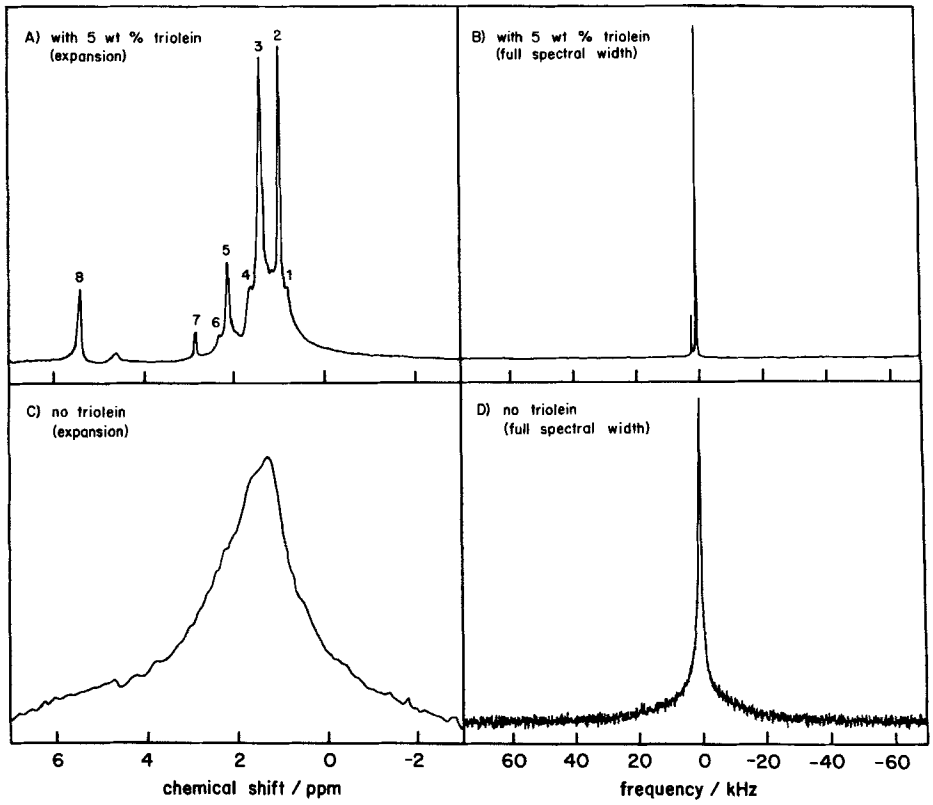

FIG. 5. Influence of triglycerides on ^{1}H NMR spectra of cholesteryl esters at body temperature. The ^{1}H NMR spectra at left are expansions of the −3 to +7 ppm frequency range containing the distinct resonances seen for arterial plaque; the full spectra are shown at right over a −70- to +70-kHz width. In (A) and (B) are shown ^{1}H NMR spectra of an anhydrous mixture of cholesteryl linoleate/cholesteryl oleate/cholesteryl palmitate (molar ratios of 10:8:2), containing 5 wt% triolein at 37°C, whose composition approximates that of human atheroma (fatty plaque). A high-resolution ^{1}H NMR spectrum is obtained at 37°C, similar to that of fatty plaque and its extracted lipids (Figs. 1 and 2), with little or no underlying broad component. In (C) and (D), ^{1}H NMR spectra are depicted at 37°C of a mixture of cholesteryl esters of the same composition, but which does not contain triolein. In the absence of triglycerides (triolein), the temperature range over which the isotropic phase is found is higher than in its presence, and broader spectra are obtained at body temperature. The results suggest that the ^{1}H NMR spectra of human atheroma at 37°C are due to a mixture of cholesteryl esters in the isotropic liquid phase.

liquid state at body temperature (37°C). Moreover, it appears that the thermotropic behavior of samples of arterial plaque as detected by ^{1}H NMR spectroscopy depends on the content of cholesteryl esters and triglycerides (*38, 46–48*), and thus can provide information on the chemical and physical properties of the atheromatous lipid molecules. Free cholesterol, on the other hand, is only sparingly soluble in cholesteryl esters (*2, 38*). It is often found in the solid or crystalline phase in atheromatous tissue (*2, 19–22*) and gives rise to broad ^{1}H NMR signals (Fig. 4H), which presumably are lost in the baseline noise.

Spin–spin (transverse) and spin–lattice (longitudinal) relaxation studies. To further characterize the atheromatous lipids, their transverse (T_2^*) and longitudinal (T_1) relaxation times were determined by ^{1}H NMR spectroscopy at different magnetic field strengths. The sharp spectral lines observed for excised atheroma and its hydrated extracted lipids (Figs. 1 and 2) were found to have approximately Lorentzian lineshapes at 37°C and higher temperatures, to within experimental error, as expected of an isotropic fluid (not shown). T_2^* relaxation times were estimated at 37°C by fitting the resolved individual resonances to Lorentzian spectral lineshapes and are summarized in Table 1. In addition, data are included for anhydrous cholesteryl linoleate in the isotropic phase, a representative cholesteryl ester found in human fatty plaque. Within experimental error, little difference is seen in the linewidths and T_2^* values of the different samples, consistent with earlier ^{13}C NMR studies (*24, 26*). Over the range of magnetic field strengths from 6.342 to 11.75 T (^{1}H frequencies of 270.0 to 500.1 MHz), the estimated linewidths and T_2^* values of the corresponding resonances are similar, suggesting that the line broadening is probably homogeneous in origin and due to molecular motions. T_1 relaxation times are also indicated in Table 1 for human atheroma, its extracted lipids, and cholesteryl linoleate at 37°C. For each of the samples investigated, the T_1 relaxation times of the resolved resonances increase significantly with increasing magnetic field strength, that is, resonance frequency (Table 1), and are consistent with earlier ^{1}H NMR studies of cholesteryl esters (*49, 50*). The T_1 values of the corresponding resonances of human fatty plaque and its extracted lipids are similar to those of cholesteryl linoleate in the isotropic phase and to those of phospholipid bilayers (*51, 52*), but are typical less than that of water in biological tissues (*36, 37*).

In general, the T_1 and T_2^* relaxation times of lipids are sensitive to the rates and types of their molecular motions (*53–57*). The observation that the T_1 relaxation times increase with both frequency (Table 1) and temperature (not shown) suggests that the motions responsible for the relaxation are more complex than in simple fluids (*53–57*). Moreover, T_2^* is substantially less than T_1, and it is likely that different motions influence the ^{1}H transverse and longitudinal relaxation rates of the atheromatous lipids, such as rapid isomerizations of the fatty acyl chains and slower anisotropic motions of the sterol rings or slowly relaxing local structures. For the sake of illustration, if it is assumed that the motions responsible for the linewidths and T_2^* values can be approximated in terms of an effective correlation time, then the viscosity η of the atheromatous lipid constituents would be similar to that of a neat cholesteryl ester in the isotropic liquid state, which is about 2 poise in the case of cholesteryl oleate (*48*). However, since $T_2^* \neq T_1$, a single bulk viscosity parameter cannot describe fully the molecular dynamics of cholesteryl esters in the isotropic phase, and a more detailed treatment is appropriate (*26, 47, 55*).

TABLE 1

Proton Spin–Spin (T_2^*) and Spin–Lattice (T_1) Relaxation Times of Lipids of Human Atheroma at Different Magnetic Field Strengths (Temperature = 37°C)[a]

Sample	Resonance[b]	δ/ppm[c]	T_2^*/ms (T)			T_1/s (T)		
			6.34[d]	8.48	11.7	6.34	8.48	11.7
Fatty plaque	2	0.87	6	6	6	0.45 ± 0.01	0.60 ± 0.01	0.75 ± 0.04
	3	1.27	7	5	6	0.44 ± 0.01	0.57 ± 0.02	0.74 ± 0.07
	5	1.99	7	6	6	0.39 ± 0.01	0.56 ± 0.03	0.72 ± 0.03
	7	2.73	8	6	8	—	0.58 ± 0.04	—
	8	5.28	7	6	6	0.59 ± 0.03	0.70 ± 0.04	0.78 ± 0.06
Extracted lipids	2	0.86	11	7	9	0.30 ± 0.02	0.45 ± 0.01	0.64 ± 0.01
	3	1.28	8	7	6	0.28 ± 0.02	0.42 ± 0.01	0.57 ± 0.02
	5	2.01	9	7	6	0.23 ± 0.02	0.38 ± 0.01	0.55 ± 0.02
	7	2.74	11	7	5	—	0.37 ± 0.03	—
	8	5.30	12	7	7	0.24 ± 0.08	0.48 ± 0.05	0.63 ± 0.04
Cholesteryl linoleate	2	0.88	—	10	—	0.53 ± 0.01	0.72 ± 0.02	—
	3	1.30	—	6	—	0.52 ± 0.01	0.68 ± 0.01	—
	5	2.11	—	8	—	0.48 ± 0.01	0.62 ± 0.01	—
	7	2.78	—	13	—	0.41 ± 0.03	0.58 ± 0.01	—
	8	5.38	—	9	—	0.60 ± 0.02	0.84 ± 0.05	—

[a] T_2^* values were estimated from fits of resolved sharp resonances to Lorentzian lineshapes using the relation $\Delta\nu = (\pi T_2^*)^{-1}$, where $\Delta\nu$ is the full width at half-height. The estimated errors of the T_2^* values are ±20%. T_1 relaxation times and errors were determined from three-parameter exponential fits of peak amplitudes of partially relaxed spectra obtained using the inversion-recovery pulse sequence (*36*).

[b] Resonance assignments are given in Fig. 1.

[c] Chemical shifts (δ) are in parts per million (ppm) relative to an external capillary containing DSS.

[d] Magnetic field strength in tesla. One tesla (T) is equal to 10^7 gauss (G).

Magnetic resonance imaging (MRI) of human arterial lesions. In NMR imaging, one applies magnetic field gradients to encode the spatial locations of protons in biological specimens—largely due to water and lipids—in the frequency and phase of their NMR signals (*36, 37*). The contrast between different tissues in NMR images is a function of at least three parameters: namely ρ, the proton density; T_1, the spin–lattice or longitudinal relaxation time; and T_2^*, the spin–spin or transverse relaxation time. In addition, chemical shift (δ) differences as well as macroscopic transport or

flow can also influence contrast. A difference in one or more of these parameters can distinguish neighboring tissues in NMR imaging (*36, 37*). Consequently, the above findings offer a possible basis for use of ^{1}H NMR to evaluate the accumulation of lipids which occurs early in atherogenesis, since different spectral lineshapes and T_2^* values are observed relative to normal arterial wall at body temperature. The T_1 values of the atheromatous lipids differ significantly from that of tissue water (*36, 37*), and may also lead to NMR image contrast. Preliminary NMR imaging studies of human atheromatous tissue have been reported (*19, 58–62*).

As discussed above, the results of ^{1}H NMR spectroscopy suggest that NMR images of human atheroma (fatty plaque) obtained at body temperature may include a contribution from cholesteryl esters in the isotropic phase, with well-resolved spectral lines. Such narrow spectral lines represent slowly decaying signals in the time domain (i.e., with relatively long apparent T_2^* values), while broad lines correspond to rapidly decaying signals (i.e., with very short apparent T_2^* values) (*43, 44*). It is important to note that T_2^* is the time constant for monoexponential decay of NMR signal intensity in the time domain, which by Fourier transformation corresponds to a Lorentzian lineshape as typically observed for liquid samples. On the other hand, T_2^* is ill-defined for broad, non-Lorentzian lineshapes, as characteristic of the solid and liquid-crystalline states (*43, 44*). The T_2^* values estimated from the linewidths of the sharp ^{1}H NMR spectral components due to atheromatous lipids are about 5–10 ms (Table 1), suggesting that significant intensity will remain with the relatively long echo times currently employed for NMR imaging (TE $\geqslant$ 10 ms). To make use of the ^{1}H NMR spectral signature of atheroma, NMR imaging methods for separating the fat and water signals can be applied; a number of schemes for chemical-shift imaging exist (*63–65*). The results of Figs. 1–2 suggest that the presence of atheromatous lipids can be identified by ^{1}H NMR, thus providing a basis for quantification of the size of the atheromatous regions. Use of shorter TE values will enable further chemical and physical information to be obtained regarding the deposits of cholesteryl esters and other lipids (*2, 19–22*). With such methods and knowledge of the spectral lineshapes as described here, one can eventually achieve quantification of the size of early atheromatous lesions and the amount of cholesteryl ester deposition in living human subjects.

We have begun to apply this knowledge to NMR imaging of excised human aortas, obtained postmortem, in which lesions containing cholesteryl esters and cholesterol with minimal obstruction of the lumen have been accurately identified. In addition, studies have been carried out of carotid artery occlusions surgically removed from living patients (endarterectomy). Through use of modern image-processing and pattern-recognition techniques, the results have been further refined and extended in a manner analogous to that used in multispectral satellite imaging, such as the LANDSAT series developed by the National Aeronautics and Space Administration (NASA) (*66*). The observation of well-resolved ^{1}H NMR spectral lines from the lipids of human atheroma illustrates clearly that the pixel intensity values convey more dimensions of information than described by the simple bulk parameters ρ, T_1, and T_2^*. From the viewpoint of image-processing and pattern-recognition methods, knowledge of the chemical and physical basis for the ^{1}H NMR spectral signature is less essential, and the data can be analyzed simply in terms of its discriminant power. Thus, by collating the series of images into a multidimensional data set, the separability of the different tissue constituents can be enhanced relative to that if only a single variable such as T_2^* is con-

sidered. Selection and combination of the base image planes can then be accomplished with use of multivariate statistical techniques (*19*) to enhance pixel separability, and thereby access the full dimensionality of the data. As a representative preliminary example, Fig. 6 shows a cross-sectional image of a human aorta produced by multivariate analysis of a set of NMR image planes obtained with different acquisition parameters. Subintimal, atheromatous lesions containing minimally raised accumulations of cholesterol and cholesteryl esters are clearly evident (left), as confirmed by subsequent ^{1}H NMR spectroscopy, chemical analysis, and pathological examination (right). Moreover, one can further distinguish among different classes of arterial constituents, including normal arterial wall, mixed fibrous lesions, calcified plaque, and adventitial fat, as shown in Fig. 7. Extension of this work to living human subjects using cardiac gating (*37*) is expected to be straightforward, and preliminary studies are currently in progress.

CONCLUSIONS

In the future, the results described here can be expected to find application in the detection and monitoring of arterial disease in living human individuals. Current

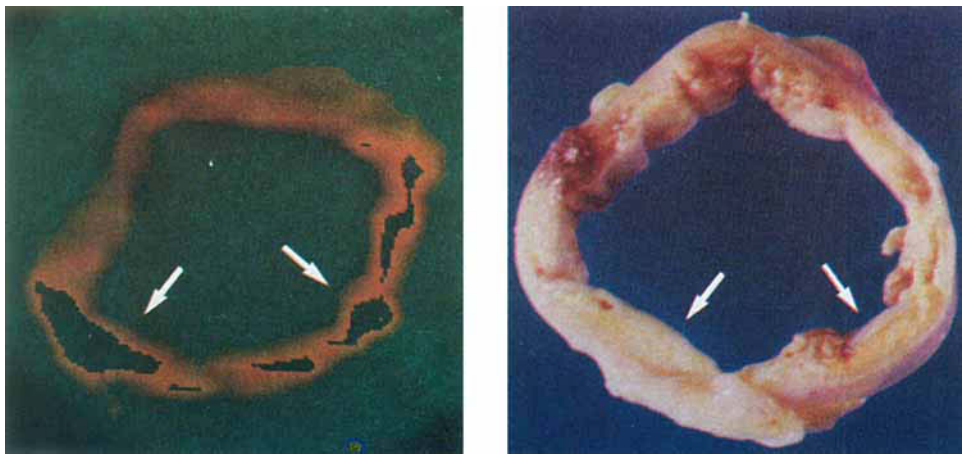

FIG. 6. Nuclear magnetic resonance (NMR) image of human atheroma *in situ*, that is, intact within the arterial wall, compared with results of gross pathology. The aorta specimen was fresh *ex vivo* at ambient temperature (23°C) and was suspended in a cylinder containing 0.9% NaCl. The left photograph shows a pseudocolor composite derived from a total of 18 spectral-, ρ-, T_1-, and T_2^*-weighted NMR images of the same cross-sectional plane; the final resolution is 1.2 mm/pixel. The false color image was produced by condensation or projection of the multidimensional data to three separate planes, which were then mapped to the individual channels of a color raster display. The location of the atheroma within the vessel wall was further highlighted by thresholding. Regions corresponding to vessel wall (orange), lumen (green), and minimally raised, subintimal fatty plaque within the vessel wall (green) are clearly evident. The right photograph shows a cross section of the same region of the same aorta, as dissected subsequent to NMR imaging. The specimen has been slightly distorted by excision, but corresponds to the same orientation as in the left photograph. In each case, regions of minimally raised atheroma within the subintimal wall are identified by arrows. The lesions represent fatty plaque, with little or no evidence of fibrosis, calcification, or lumenal narrowing. The results show that NMR imaging can accurately display early atheroma confined within the wall of the human aorta.

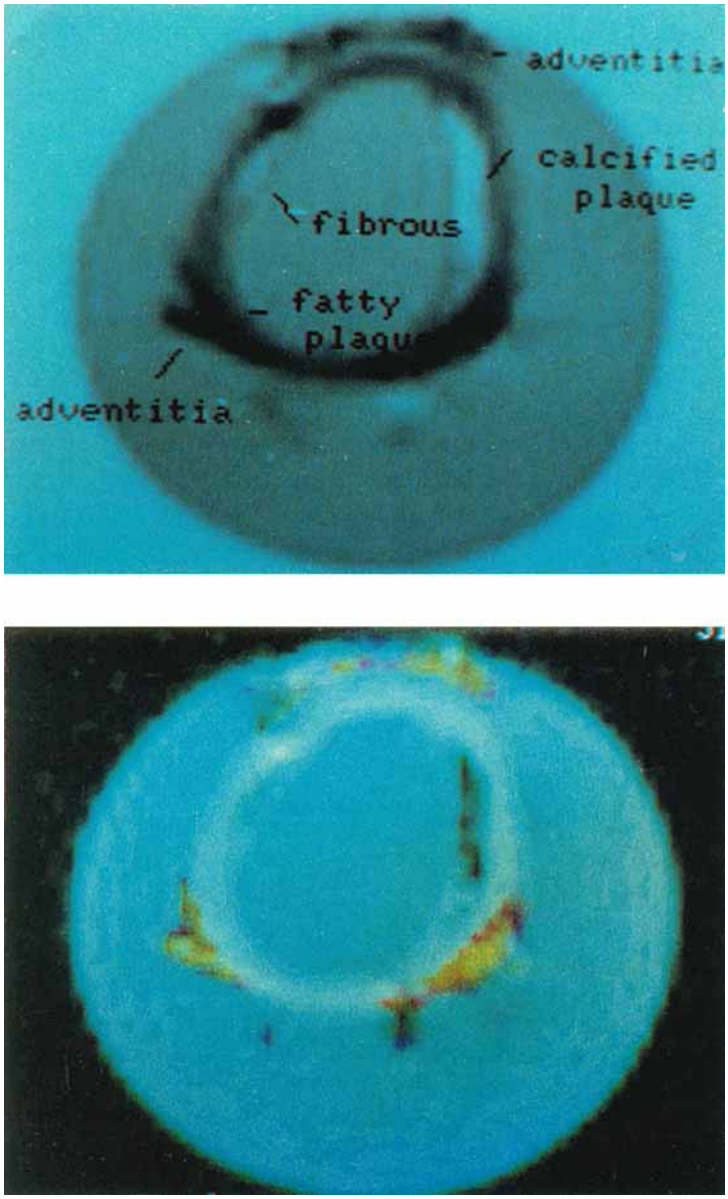

FIG. 7. False color composites of an excised human aorta obtained by multivariate analysis of cross-sectional NMR image planes at 23°C, showing evidence of later atheromatous lesions. The instrumental resolution is 0.6 mm/pixel. Regions of normal aortic wall are distinguished from vessel lumen; fatty, fibrous, and calcified plaque; and adventitial fat, as indicated in the top photograph. The bottom photograph shows a false color image of the same cross-sectional plane, in which calcified plaque appears dark and adventitial fat as yellow. Note that a simple fat-selective image highlights adventitial fat, which could be mistaken for subintimal atheroma at low spatial resolution.

methods utilizing angiography for these purposes are invasive, are of possible detriment to health, and are ill-suited and impractical for serial monitoring of individuals or human populations. As a result, prevalent strategies for therapeutic intervention have tended to rely on reduction or elimination of risk factors shown from epidemiological studies (*8*) and clinical trials (*9, 10*) to be correlated with cardiovascular disease due to atherosclerosis. Recently, drugs (mevinolin and synvinolin) have been introduced which act by inhibiting HMG CoA reductase, a key enzyme which catalyzes the committed step of cholesterol biosynthesis. When used alone or in combination with bile acid binding resins such as cholestyramine, these reductase inhibitors can be quite effective in the lowering of total and LDL serum cholesterol levels (*6, 7*). The value of these and other regimens would be enhanced by accurate serial evaluation of their specific biological effects *in vivo*. Together with risk factor reduction, for example, through behavioral, diet or drug therapy, the results described here offer the potential for preventive treatment of early arterial disease in individual patients. We have demonstrated that information regarding the chemical and physical state of the lipids of human arterial plaque can be obtained through use of ^{1}H NMR spectroscopy. This knowledge provides a necessary and sufficient basis for eventual development of tests for diagnosis of early atheroma within the walls of the human aorta and other blood vessels. In conjunction with NMR imaging, the present results can be used to detect and quantify potentially reversible atheromatous disease, so that tissue responses can be monitored on an individual basis, and therapy adjusted until benefit is realized. In this manner, it may be possible to follow the progression of arterial plaque lipid deposition, and thus hopefully to reduce the leading cause of death in the United States and other industrial nations—that is, by focused medical treatment during the clinically silent, early stages of atherogenesis.

ACKNOWLEDGMENTS

We thank Wayne Cail, Milan DiPierro, Jeffrey Ellena, John Mugler, Amir Salmon, Vladimir Sklenar, Kuldeep Teja, and Theodore Trouard for their assistance and valuable advice. This research was funded in part by NIH Grant HL 07355 (C.R.A.), the Whitaker Foundation (M.B.M., J.R.B.), NIH Grant EY 03754 (M.F.B.), and the Thomas F. Jeffress and Kate Miller Jeffress Memorial Trust (M.F.B.). M.F.B. is the recipient of a Research Career Development Award from the NIH and is an Alfred P. Sloan Research Fellow.

REFERENCES

1. R. I. LEVY, *Arteriosclerosis* **1,** 312 (1981).
2. D. M. SMALL AND G. G. SHIPLEY, *Science* **185,** 222 (1974).
3. R. ROSS AND J. A. GLOMSET, *New Engl. J. Med.* **295,** 369 (1976).
4. R. ROSS AND J. A. GLOMSET, *New Engl. J. Med.* **295,** 420 (1976).
5. R. ROSS, *New Engl. J. Med.* **314,** 488 (1986).
6. M. S. BROWN AND J. L. GOLDSTEIN, *Sci. Amer.* **251,** 58 (1984).
7. M. S. BROWN AND J. L. GOLDSTEIN, *Science* **232,** 34 (1986).
8. W. B. KANNEL, W. P. CASTELLI, T. GORDON, AND P. M. MCNAMARA, *Ann. Int. Med.* **74,** 1 (1971).
9. Lipid Research Clinics Program, *J. Amer. Med. Assoc.* **251,** 351 (1984).
10. Lipid Research Clinics Program, *J. Amer. Med. Assoc.* **251,** 365 (1984).
11. T. J. PETERS AND C. DE DUVE, *Exp. Mol. Pathol.* **20,** 228 (1974).
12. A. R. TALL, D. ATKINSON, D. M. SMALL, AND R. W. MAHLEY, *J. Biol. Chem.* **252,** 7288 (1977).
13. D. J. GORDON, K. M. SALZ, K. J. ROGGENKAMP, AND F. A. FRANKLIN, JR., *Arteriosclerosis* **2,** 537 (1982).

14. W. S. HARRIS, W. E. CONNER, AND M. P. MCMURRY, *Metabolism* **32,** 179 (1983).
15. J. A. GLOMSET, *New Engl. J. Med.* **312,** 1253 (1985).
16. D. KROMHOUT, E. B. BOSSCHIETER, AND C. DE LEZENNE COULANDER, *New Engl. J. Med.* **312,** 1205 (1985).
17. B. E. PHILLIPSON, D. W. ROTHROCK, W. E. CONNOR, W. S. HARRIS, AND D. R. ILLINGWORTH, *New Engl. J. Med.* **312,** 1210 (1985).
18. T. H. LEE, R. L. HOOVER, J. D. WILLIAMS, R. I. SPERLING, J. RAVALESE III, B. W. SPUR, D. R. ROBINSON, E. J. COREY, R. A. LEWIS, AND K. F. AUSTEN, *New Engl. J. Med.* **312,** 1217 (1985).
19. J. D. PEARLMAN, "MRI of Human Atheroma: NMR Spectral Signatures of Liquid Crystals in Human Atheroma as a Basis for Multidimensional Digital Imaging of Atherosclerosis," Ph.D. thesis, University of Virginia (1986).
20. S. S. KATZ, G. G. SHIPLEY, AND D. M. SMALL, *J. Clin. Invest.* **58,** 200 (1976).
21. E. B. SMITH AND R. S. SLATER, *Atherosclerosis* **15,** 37 (1972).
22. B. LUNDBERG, *Atherosclerosis* **56,** 93 (1985).
23. R. G. M. DUFFIELD, B. LEWIS, N. E. MILLER, C. W. JAMIESON, J. N. H. BRUNT, AND A. C. F. COLCHESTER, *Lancet* **2,** 639 (1983).
24. J. A. HAMILTON, E. H. CORDES, AND C. J. GLUECK, *J. Biol. Chem.* **254,** 5435 (1979).
25. R. J. CUSHLEY, B. J. FORREST, A. K. GROVER, AND S. R. WASSALL, *Canad. J. Biochem.* **58,** 206 (1980).
26. P. A. KROON, D. M. QUINN, AND E. H. CORDES, *Biochemistry* **21,** 2745 (1982).
27. J. M. STEIM, O. J. EDNER, AND F. G. BARGOOT, *Science* **162,** 909 (1968).
28. R. B. LESLIE, D. CHAPMAN, AND A. M. SCANU, *Chem. Phys. Lipids* **3,** 152 (1969).
29. D. CHAPMAN, R. B. LESLIE, R. HIRZ, AND A. M. SCANU, *Biochim. Biophys. Acta* **176,** 524 (1969).
30. E. G. FINER, R. HENRY, R. B. LESLIE, AND R. N. ROBERTSON, *Biochim. Biophys. Acta* **380,** 320 (1975).
31. B. SEARS, R. J. DECKELBAUM, M. J. JANIAK, G. G. SHIPLEY, AND D. M. SMALL, *Biochemistry* **15,** 4151 (1976).
32. J. A. HAMILTON AND E. H. CORDES, *J. Biol. Chem.* **253,** 5193 (1978).
33. P. A. KROON, *J. Biol. Chem.* **256,** 5332 (1981).
34. P. A. KROON AND M. KRIEGER, *J. Biol. Chem.* **256,** 5340 (1981).
35. P. A. KROON AND J. SEIDENBERG, *Biochemistry* **21,** 6483 (1982).
36. D. G. GADIAN, "Nuclear Magnetic Resonance and Its Applications to Living Systems," Oxford Univ. Press (Clarendon), London/New York, 1982.
37. P. G. MORRIS, "Nuclear Magnetic Resonance Imaging in Medicine and Biology," Oxford Univ. Press (Clarendon), London/New York, 1986.
38. D. M. SMALL, *in* "Surface Chemistry of Biological Systems" (M. Blank, Ed.), p. 55, Plenum, New York, 1970.
39. D. M. ENGELMAN AND G. M. HILLMAN, *J. Clin. Invest.* **58,** 997 (1976).
40. G. M. HILLMAN AND D. M. ENGELMAN, *J. Clin. Invest.* **58,** 1008 (1976).
41. D. CHAPMAN AND A. MORRISON, *J. Biol. Chem.* **241,** 5044 (1966).
42. N. S. BHACCA AND D. H. WILLIAMS, "Applications of NMR Spectroscopy in Organic Chemistry Illustrations from the Steroid Field," Holden-Day, San Francisco, 1964.
43. H. WENNERSTRÖM AND G. LINDBLOM, *Quart. Rev. Biophys.* **10,** 67 (1977).
44. M. BLOOM, E. E. BURNELL, A. L. MACKAY, C. P. NICHOL, M. I. VALIC, AND G. WEEKS, *Biochemistry* **17,** 5750 (1978).
45. C. BURKS AND D. M. ENGELMAN, *Proc. Natl. Acad. Sci. USA* **78,** 6863 (1981).
46. R. J. DECKELBAUM, G. G. SHIPLEY, AND D. M. SMALL, *J. Biol. Chem.* **252,** 744 (1977).
47. D. H. CROLL, D. M. SMALL, AND J. A. HAMILTON, *Biochemistry* **24,** 7971 (1985).
48. J. A. HAMILTON, N. OPPENHEIMER, AND E. H. CORDES, *J. Biol. Chem.* **252,** 8071 (1977).
49. C. R. DYBOWSKI AND C. G. WADE, *J. Chem. Phys.* **55,** 1576 (1971).
50. R. M. C. MATTHEWS AND C. G. WADE, *J. Magn. Reson.* **19,** 166 (1975).
51. P. A. KROON, M. KAINOSHO, AND S. I. CHAN, *Biochim. Biophys. Acta* **433,** 282 (1976).
52. M. F. BROWN, G. P. MILJANICH, AND E. A. DRATZ, *Biochemistry* **16,** 2640 (1977).
53. M. F. BROWN, *J. Chem. Phys.* **77,** 1576 (1982).
54. M. F. BROWN, A. A. RIBEIRO, AND G. D. WILLIAMS, *Proc. Natl. Acad. Sci. USA* **80,** 4325 (1983).
55. M. F. BROWN, *J. Chem. Phys.* **80,** 2808 (1984).
56. M. F. BROWN, *J. Chem. Phys.* **80,** 2832 (1984).
57. M. F. BROWN, J. F. ELLENA, C. TRINDLE, AND G. D. WILLIAMS, *J. Chem. Phys.* **84,** 465 (1986).

58. L. KAUFMANN, L. E. CROOKS, P. E. SHELDON, W. ROWAN, AND T. MILLER, *Invest. Radiol.* **17,** 554 (1982).
59. R. J. HERFKENS, C. B. HIGGINS, H. HRICAK, M. J. LIPTON, L. E. CROOKS, P. LANZER, E. BOTVINICK, B. BRUNDAGE, P. E. SHELDON, AND L. KAUFMAN, *Radiology* **147,** 749 (1983).
60. R. J. HERFKENS, C. B. HIGGINS, H. HRICAK, M. J. LIPTON, L. E. CROOKS, P. E. SHELDON, AND L. KAUFMAN, *Radiology* **148,** 161 (1983).
61. K. SOILA, P. NUMMI, T. EKFORS, M. VIAMONTE, AND M. KORMANO, *Invest. Radiol.* **21,** 411 (1986).
62. G. E. WESBEY, C. B. HIGGINS, J. D. HALE, AND P. E. VALK, *Cardiovasc. Intervention Radiol.* **8,** 342 (1986).
63. W. T. DIXON, *Radiology* **153,** 189 (1984).
64. J. FRAHM, A. HAASE, W. HAENICKE, D. MATTHAEI, H. BOMSDORF, AND T. HELZEL, *Radiology* **156,** 441 (1985).
65. D. KUNZ, *Magn. Reson. Med.* **3,** 639 (1986).
66. M. W. VANNIER, R. L. BUTTERFIELD, D. JORDAN, W. A. MURPHY, R. G. LEVITT, AND M. GADO, *Radiology* **154,** 221 (1985).